Temporal features of size constancy for perception and action in a real-world setting: A combined EEG-kinematics study

Simona Noviello [a], Saman Kamari Songhorabadi [a], Zhiqing Deng [b], Chao Zheng [b], Juan Chen [b,c], Angelo Pisani [d], Elena Franchin [a], Enrica Pierotti [f], Elena Tonolli [f], Simona Monaco [f], Louis Renoult [e], Irene Sperandio [a,*]

[a] Department of Psychology and Cognitive Science, University of Trento, Rovereto, TN, Italy
[b] School of Psychology, South China Normal University, Guangzhou, Guangdong Province, China
[c] Philosophy and Social Science Laboratory of Reading and Development in Children and Adolescents (South China Normal University), Ministry of Education, China
[d] Department of Psychology "Renzo Canestrari", University of Bologna, Italy
[e] School of Psychology, University of East Anglia, Norwich, UK
[f] Center for Mind/Brain Sciences (CIMeC), University of Trento, Rovereto, TN, Italy

ARTICLE INFO

ABSTRACT

A stable representation of object size, in spite of continuous variations in retinal input due to changes in viewing distance, is critical for perceiving and acting in a real 3D world. In fact, our perceptual and visuo-motor systems exhibit size and grip constancies in order to compensate for the natural shrinkage of the retinal image with increased distance. The neural basis of this size-distance scaling remains largely unknown, although multiple lines of evidence suggest that size-constancy operations might take place remarkably early, already at the level of the primary visual cortex. In this study, we examined for the first time the temporal dynamics of size constancy during perception and action by using a combined measurement of event-related potentials (ERPs) and kinematics. Participants were asked to maintain their gaze steadily on a fixation point and perform either a manual estimation or a grasping task towards disks of different sizes placed at different distances. Importantly, the physical size of the target was scaled with distance to yield a constant retinal angle. Meanwhile, we recorded EEG data from 64 scalp electrodes and hand movements with a motion capture system. We focused on the first positive-going visual evoked component peaking at approximately 90 ms after stimulus onset. We found earlier latencies and greater amplitudes in response to bigger than smaller disks of matched retinal size, regardless of the task. In line with the ERP results, manual estimates and peak grip apertures were larger for the bigger targets. We also found task-related differences at later stages of processing from a cluster of central electrodes, whereby the mean amplitude of the P2 component was greater for manual estimation than grasping. Taken together, these findings provide novel evidence that size constancy for real objects at real distances occurs at the earliest cortical stages and that early visual processing does not change as a function of task demands.

1. Introduction

Size constancy, the scaling mechanism that allows us to perceive an object as having the same size regardless of changes in viewing distance, is a remarkable ability of the human brain. By integrating retinal image and distance information, the visual system achieves a stable and coherent representation of object size despite the ever-changing retinal projections (for a review, see Sperandio and Chouinard, 2015). An accurate representation of size is crucial, not only for perceptual

recognition, but also for goal-directed actions, such as grasping. In fact, when we reach out to pick up an object, our grip aperture is scaled to the true size of the object irrespective of viewing distance. In other words, our visuomotor system shows grip constancy (Chen et al., 2018; Kudoh et al., 1997; Marotta et al., 1997; Niechwiej-Szwedo et al., 2022; Servos et al., 1992; Whitwell et al., 2020). When and where the brain achieves size (or grip) constancy is one of the most fascinating questions in visual neuroscience.

It is well established that the primary visual cortex (V1), the first

cortical stage of processing of visual information, contains a precise retinotopic map of the visual inputs such that adjacent parts of the visual field activate adjacent parts of the cortex (Glickstein and Whitteridge, 1987; Holmes, 1918; Tootell et al., 1982). It has been assumed that this topographic map of retinal projections is a hallmark of V1 organization and constitutes the core element of our representations of the real world. However, converging evidence on active visual processes in V1 now challenges this view. FMRI studies in humans using visual illusions have demonstrated that the spatial extent of neural activation in V1 reflects the perceived rather than the retinal size of an object (Fang et al., 2008; Murray et al., 2006; Pooresmaeili et al., 2013; Schwarzkopf et al., 2011; Schwarzkopf and Rees, 2013; Weidner et al., 2014). Likewise, Sperandio and colleagues (Sperandio et al., 2012) using real depth cues have reported even greater modulations in V1 activity, than those observed with visual illusions, by systematically manipulating the real distance of a stimulus of fixed retinal image size. The involvement of V1 in size constancy operations has been further corroborated by single-cell studies in the monkey (Ni et al., 2014) and epileptic patients (Marg and Adams, 1970; Smith and Marg, 1975), showing that the firing profile of some V1 neurons is more compatible with the perceptual outcome than the retinal stimulation. Importantly, there is also evidence in the monkey that oculomotor adjustments that are made in response to changes in viewing distance, such as vergence and accommodation, can modulate the activity of V1 neurons (Dobbins et al., 1998; Trotter et al., 1992, 2004; Trotter and Celebrini, 1999). Taken together, these findings indicate that perceived object size can be represented in the neural activity of V1 and open up the possibility that size-distance integration might take place in the initial processing of V1 or even earlier. However, our recent ERP study (Chen et al., 2019a; b) on size constancy, in which we presented circles of different physical sizes on a movable monitor that was placed either near or far from the observer's eyes, failed to show modulations of the earliest visual components in response to perceived size. Surprisingly, we observed instead that the integration of distance information and retinal image size took about 150 ms to unfold. This suggests that the size-constancy-related patterns of activity in V1 described in the abovementioned fMRI studies might not be locally generated in V1, but rather they might reflect feedback activity from higher-level cortical areas.

In the current investigation, we examined for the first time the temporal features of the neural processes underlying size constancy for perception and action by combining EEG and kinematics recordings. Notably, we went one step further with respect to our previous ERP study in terms of ecological validity of our paradigm and used real 3D stimuli, rather than 2D flat pictures, such that participants could also physically interact with the target objects. In doing so, we had to reduce our experimental conditions to only two critical conditions, namely small-near and big-far, where disks of different physical size were placed at different distances in order to subtend the same retinal angle. This manipulation allowed us to test directly if stimuli of different physical sizes were processed in relation to their perceived or retinal size (Holway and Boring, 1941; Sperandio et al., 2009). Crucially, we believe that the perceptual scaling of size invoked by real objects at real distances can better capture size constancy mechanisms as they operate in the real world (Snow and Culham, 2021). As such, we expect to find an earlier integration of retinal image and distance cues using a more ecological setting with respect to what was reported in Chen et al.'s study (2019b).

2. Methods

2.1. Participants

Sixteen healthy volunteers (12 females and 4 males; $M_{age} = 23.75$ years, SD = 3.38, range = 20–33 years old) were enrolled in the study. To determine our sample size, we referred to a previous EEG study on size constancy by Chen et al. (Chen et al., 2019a,b). Participants were mostly students or workers at the University of Trento (Italy) and were

reimbursed 10 euros per hour for their time. Participants were recruited using an advertisement posted on major social media, such as Facebook and WhatsApp. All participants were right-handed, with normal or corrected-to-normal vision (only glasses prescription and no contact lenses were allowed), and with no history of neurological or psychiatric disorders. Before volunteers were deemed eligible for participation, we asked them to measure their arm's length from the shoulder to the wrist as well as their head circumference. The arm's measurement was required to ensure that participants would be able to reach the furthest position of the stimulus comfortably; the head circumference measurement was required to ensure that it would match the available size of the EEG cap. For both arm's length and head circumference, the minimum measurement required was 55 cm. Written informed consent was obtained by all participants prior to testing. The study was conducted according to the ethical guidelines and with the approval of the Research Ethics Committee of the University of Trento.

2.2. Apparatus and materials

The main apparatus consisted of a wooden board with tracks on which we placed a white panel that could be slid near (26 cm) or far (52 cm) from the participants' eyes. A chin rest was screwed to the side of the board closest to the participant. In the center of the board, a small squared magnet was used to attach the stimuli (real 3D disks) and served as a fixation point. Stimuli were 3D printed and consisted of two disks with a thickness of 0,5 cm and a diameter of 4 cm (small) and 8 cm (big). As in Chen et al. (2019a,b), black stimuli (luminance = 2.10 cd/m2) were presented against a white background (luminance = 50,47 cd/m2), so that changes in retinal illuminance with distance were minimized. The two disks had a metal plate glued on the backside that allowed us to magnetically attach them to the movable panel. Crucially, the small stimulus was always presented at the near distance, whereas the big stimulus was always positioned at the far distance in order to subtend the same visual angle (8.8°) on the retina. To control for the exposure duration of the stimuli, we used a Polymer Dispersed Liquid Crystal (PDLC) device that could become opaque or transparent according to corresponding triggers sent by a custom-made code in MATLAB (https://www.mathworks.com/products/matlab.html). The PDLC screen was the size of an A4 sheet (21 cm × 29.7 cm) and it was attached to the chin rest 10 cm away from the participant's face in order to achieve the least interference on the EEG signal. A numeric keypad was placed on the table next to the wooden board, on the right, and the Insert key was marked with tape to indicate which key participants had to press with their thumb and index finger during the experimental procedure (Fig. 1).

2.3. EEG recording

Scalp EEG was collected using a g.tec medical engineering GmbH (Austria) recording system. Fifty-nine Ag/AgCl active electrodes (g. SCARABEO) were inserted into a flexible nylon cap provided with labeled holder rings, according to the international 10–20 system. For the EEG data acquisition, we used the g.HIAMP biosignal amplifier and the g.RECORDER software. The 59 electrodes included: Fp1, Fpz, Fp2, AF3, AFz, AF4, F7, F5, F3, F1, Fz, F2, F4, F6, F8, FT7, FC5, FC3, FC1, FC2, FC4, FC6, FT8, T7, C5, C3, C1, Cz, C2, C4, C6, T8, Tp7, CP5, CP3, CP1, CPz, CP2, CP4, CP6, TP8, P7, P5, P3, P1, Pz, P2, P4, P6, P8, PO7, PO3, POz, PO4, PO8, O1, Oz, O2, and Iz. Impedance was kept below 30 kΩ and regularly checked during the experiment. The ground was installed in the FCz position of the cap, the reference was placed on the Fp2 electrode and then re-referenced to the average of all the electrodes. The EEG signal was amplified by 500 K, band pass filtered at 0.05–100 Hz, and sampled at a rate of 512 Hz.
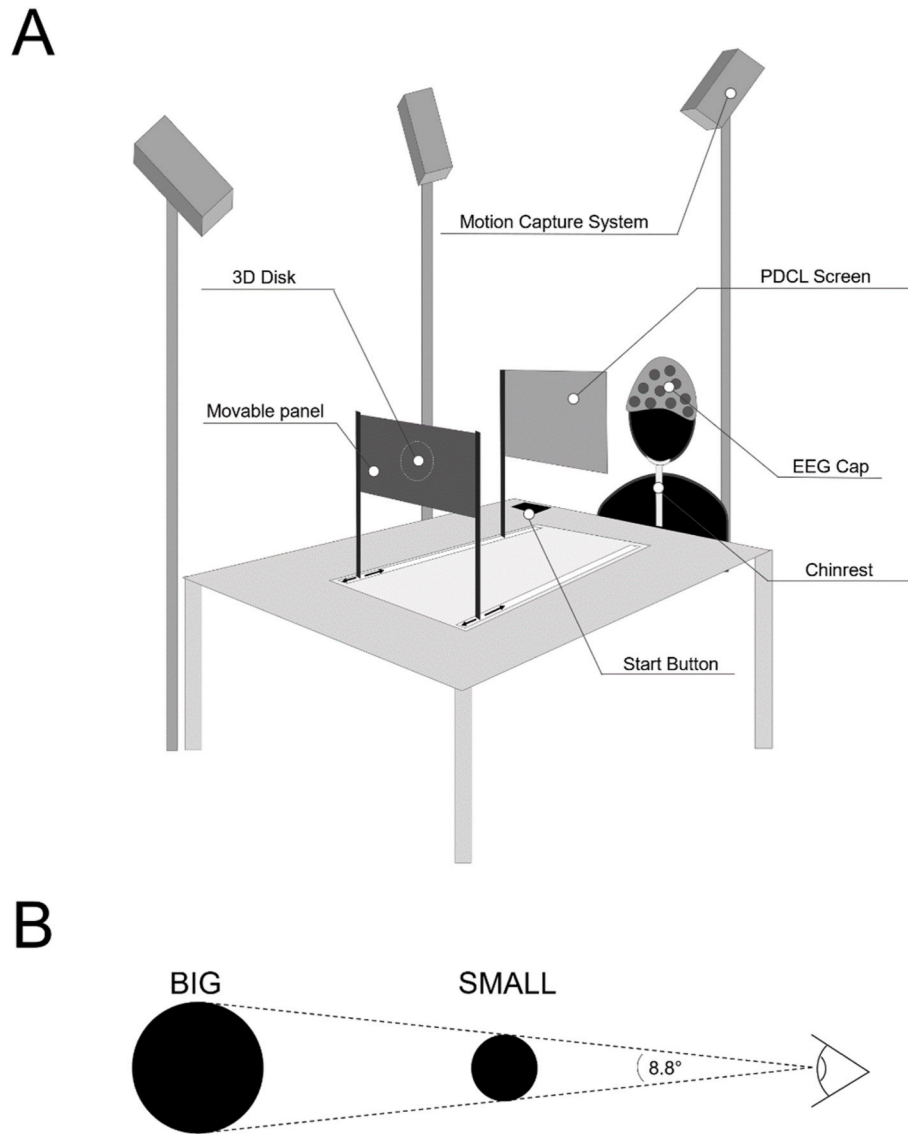
Fig. 1. A) Experimental apparatus. A wooden board was placed on a table in front of the participant. The panel, where the stimuli were placed, could be slid in the near or far position. Stimuli were magnetically attached to the panel. A Polymer Dispersed Liquid Crystal (PDLC) screen was used to control for the exposure duration of the stimuli; B) Disks of two sizes (small: 4 cm; big: 8 cm) were placed at two distances (near: 26 cm; far: 52 cm) in order to subtend the same visual angle of 8.8°.

2.4. Kinematic recording

For kinematics data acquisition, we used the Qualisys motion capture system (Qualisys AB, Gothenburg, Sweden). The setup included a multi-camera system of five ProReflex MCUs (Motion Capture Units), controlled from a central computer on which the Qualisys Track Manager software was installed. The cameras worked in combination with five reflective markers applied on the participants' right hand to track its movements. Five super-spherical markers of 6.5 mm were placed on the right hand of the participant with a double-sided tape: one on the edge of the thumb nail, one on the edge of the forefinger nail, and three arranged in a row on a Velcro wristband that participants had to wear on the wrist. The 3D position of the hand was captured with a sampling rate of 60 Hz for 4 s from the onset of each trial.

2.5. Procedure

Before the beginning of the experiment, participants were asked to fill in an abbreviated Italian version of the Edinburgh Handedness Questionnaire (adapted from Oldfield, 1971) as well as a brief demographic survey. Then, the EEG cap and the reflective markers were positioned on the participants. After that, participants were asked to sit comfortably in front of a table on which the experimental apparatus was placed with their head fixed on a chin rest and maintain fixation on a small magnet located at the center of the panel. The study was performed in an evenly lit room. Participants were instructed to complete two tasks: manual size estimation and grasping. In the manual estimation task, they were asked to manually indicate the perceived size of the disk by opening their forefinger and thumb a matching amount. In the grasping task, they were required to reach out and pick up the disk in a 'natural manner' with their thumb and forefinger.

All participants took part in two experimental sessions of approximately 3 h each, distributed on different days to prevent excessive fatigue. Each session comprised 10 blocks (5 manual estimation and 5 grasping) and each block included 40 trials divided into 20 small-near and 20 big-far conditions. Therefore, we tested 20 blocks over the two sessions for a total of 800 trials. The presentation order of the blocks as well as the conditions within each block was randomized. To allow participants to familiarize themselves with the task instructions, a few practice trials were given before testing began.

Before each block, participants were informed about which task they had to perform (i.e., manual estimation or grasping). At the beginning of each trial, participants were instructed to hold down the Insert key on the keyboard with their thumb and forefinger pinched together. The PDLC screen was opaque so that participants could not see anything in front of them. This allowed the experimenter to displace the panel at a specified viewing distance (near or far). Once the panel was correctly positioned, the PDLC screen was opened (i.e., became transparent) for 300 ms and closed again. During this time, participants saw the panel without the stimulus and had to keep their gaze steady on the fixation point. No response was required at this point. The brief opening of the screen represented our baseline condition. Then, when the screen was closed (opaque) again, the experimenter secured the stimulus to the panel according to the viewing condition: a small or a big disk if the panel was in the near or in the far distance, respectively. Once the disk was correctly placed, the screen was opened a second time. The participant saw the panel with the stimulus and had to perform the task specified at the beginning of the run. As soon as participants released the button, the screen shut down. This prevented participants from seeing their hand and/or the target stimulus during the execution of the movement and, therefore, they could not make any online adjustments based on visual feedback ('open loop', e.g., Chen et al., 2018; Hu et al., 1999; Hu and Goodale, 2000). After completing the task, they had to return to the starting position (Fig. 2). To provide the same haptic feedback about the disk size that was available for the grasping task, participants were asked to hold the object with their right hand before returning to the start position in the first 20% of trials (8) during the manual estimation blocks.

2.6. Pre-processing of EEG data

For the offline analysis, we used EEGLAB (Delorme and Makeig, 2004) and ERPLAB (Lopez-Calderon and Luck, 2014) to do the data pre-processing. Before filtering the data, we detected and interpolated the bad channels with the spherical method in EEGLAB. The continuous EEG was filtered with the IIR Butterworth filter from ERPLAB, with a high-pass filter of 0.1 Hz and a low-pass filter of 30 Hz. Next, an

Independent Component Analysis (ICA) (Stone, 2002) was performed in EEGLAB using the infomax ICA algorithm of Bell and Sejnowski (1995) to remove the artifactual components in the signal. Independent components (ICs) were classified by means of visual inspection and the IClabel plugin (Pion-Tonachini et al., 2019). Then, based on their scalp map and frequency, we removed the components representing eye- or muscle-related artifacts. Data was then re-referenced to the average of all the electrodes. After that, we extracted the epochs from −100 ms to 300 ms from the stimulus onset, using the pre-stimulus period for the baseline correction. At this point, we did an artifact detection on the epoched data using the Moving Window Peak-to-Peak Function in ERPLab, with a voltage threshold of 100 µV, and the visual inspection of the data. Finally, we computed the event-related potentials (ERPs) on the final dataset averaged across trials for each condition.

2.7. Pre-processing of kinematic data

For the analysis of kinematics, we used the QTM (Qualisys Track Manager) Software combined with a custom-made code in Matlab. Three indices of interest were extracted from the kinematic data: Manual Estimation (ME), Peak Grip Aperture (PGA), and Peak Hand Velocity (PHV). For the estimation task, ME was calculated as the distance between the two markers on the thumb and forefinger that participants held for a few seconds to indicate the perceived size of the stimulus. For the grasping task, the largest aperture achieved during the reach-to-grasp movement before making contact with the object, that is the PGA, was used as a kinematic measure of how well participants scaled the grip aperture according to the size of the object (Jeannerod, 1984). Finally, we collected the reaction time (i.e., button-release time) from the moment the screen was opened to the moment the participants started the hand movement with Psychtoolbox (Brainard, 1997; Kleiner et al., 2007; Pelli, 1997).

2.8. Statistical analysis

For the ERP analysis, electrodes of interest were selected based on maximum voltage in the grand averages in each condition. To identify
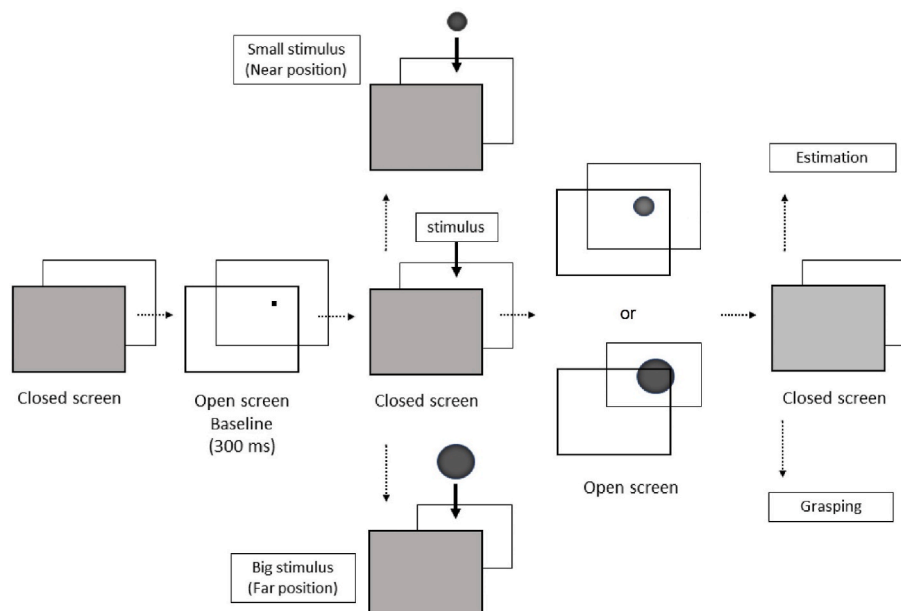

Fig. 2. Example of trial timing. This diagram represents the sequence of events during each trial. First, the experimenter received a cue indicating object size and distance for that particular trial and positioned the board at the specified distance. Then, the PDLC screen was opened for 300 ms to show the participant the fixation point and the distance at which the stimulus will be located (baseline). Once the stimulus was positioned, the screen was opened a second time signaling the participant to start the response. The initiation of the movement, with the consequent release of the starting button, caused the screen to close so that the participant performed the action in open loop (i.e., without visual feedback of the hand and/or the target object).

electrodes of interest, topographic maps of the ERP response on the scalp were created, considering the mean peak latency for the early visual components of P1, N1 and P2. A temporal window of ± 20 ms around the mean peak latency was then defined. To identify electrodes of interest, we created the topographic 3D scalp maps of the ERP response in each experimental condition during specific temporal windows, corresponding to the latencies of the grandaverage ERP components: 50–80 ms; 80–120 ms; 130–180 ms; 180–250 ms. Scalp maps of mean amplitudes within these temporal windows were then created for each condition using ERPLAB (Lopez-Calderon and Luck, 2014). From these scalp maps, six electrodes of interest were identified as being the most active in every condition. These electrodes corresponded to: P1-PZ-P2-PO3-POz-PO4 (i.e., posterior cluster). It should be noted that our selection of electrodes is similar to the one reported in the previous ERP study on size constancy by Chen et al. (2019a,b).

To better highlight differences invoked by the task, we also performed an additional analysis with a different selection of electrodes of interest. This new cluster of electrodes was identified in the topographic map generated by subtracting grasping trials from manual estimation trials. To build the scalp maps, the same approach as described above was used. The additional electrodes of interest included Cz-CP1-CPz-CP2 (i.e., central cluster). As the activity did not substantially change within each cluster of electrodes, the following ERP results on amplitude and latency refer to the average activities of each cluster sites.

The mean amplitude and the peak latency of each component were computed for each condition and each participant. A 2 × 2 repeated-measures analysis of variance (ANOVA) with Task (manual estimation vs. grasping) and Size (small vs. big) as main factors was performed on amplitudes and latencies of the early visual components. It should be noted that a significant effect of Size is indicative of size constancy as the small-near and big-far disks had the same size on the retina. Post-hoc pairwise comparisons with Bonferroni correction were performed to further investigate any significant interactions. To identify intervals with significant differences between two time courses, paired-sample t-tests were conducted point-by-point. P-values were corrected using a cluster-based test statistic (Monte Carlo method) embedded in Fieldtrip toolbox (Oostenveld et al., 2011).

For the analysis of the kinematic data, mean and standard deviation of the PGAs and MEs were calculated for both size conditions (small and big). Data was submitted to a 2 × 2 repeated measures ANOVA to evaluate the effects of Task (manual estimation vs. grasping) and Size (small vs. big) on mean and standard deviation. Post-hoc pairwise comparisons with Bonferroni correction were performed to investigate any significant interactions in more detail. To assess for size constancy, a linear regression analysis relating stimulus size and grip aperture was carried out to calculate the slope, which reflects the scaling of the opening of the hand with stimulus size (Niechwiej-Szwedo et al., 2022). We then compared the two slope values using a paired sample t-test. In addition, only for the grasping, we considered Peak Hand Velocity (PHV), which was measured during the reaching phase as the maximum speed value expressed in mm/s along the depth direction. We calculated the mean of PHV for the small (near) and the big (far) stimulus conditions. We then compared the two size conditions using a paired sample t-test. To reveal any differences in the planning phase of the movement, the mean reaction time (RT) for each condition was also calculated. Outliers were detected using Rosner's test (Rosner, 1975) and removed from the analysis. The resulting RTs underwent the same two-way ANOVA as described above.

To examine if parameters of the ERPs could predict individual differences in size constancy in perception and action, amplitudes of P1, N1, and P2 components were correlated with the kinematic measures. To provide measures of individual size-distance scaling and allow meaningful comparisons across participants, data of MEs and PGAs as well as mean amplitudes were first normalized. We, therefore, computed a "scaling index" (i.e., SI), as follows: (big condition – small condition)/ (big condition + small condition) (Chouinard et al., 2013, 2016;

Sperandio et al., 2013). Pearson correlation coefficients (r) were calculated between these indexes, and significance was established using one-tailed criteria, as we expected to observe a positive relationship between ERP and behavioural scaling indexes.

Statistical analyses were performed using the Statistical Package for Social Sciences (SPSS; IBM Corporation; Armonk, NY, USA) version 27.

3. Results

3.1. ERP results

3.1.1. ERP results from the posterior cluster

A 2 × 2 repeated-measures ANOVA was conducted on the peak latency and mean amplitude of the P1, N1 and P2 components, with Size (small vs. big) and Task (manual estimation vs. grasping) as the main factors. As can be seen in the grand-average waveforms (Fig. 3A), the neural response elicited by the big stimulus was earlier and bigger than the one evoked by the small disk. In fact, the ANOVA revealed a main effect of Size on both the peak latency and the mean amplitude of all the ERP components taken into account. The difference in amplitude between big and small conditions is illustrated in Fig. 3B. The difference waveform had a peak latency of 90 ms, while the onset latency of this difference, quantified as the time at which the voltage reached 50% of the peak amplitude (i.e., fractional peak latency, see Kiesel et al., 2008), corresponded to 51 ms after stimulus onset. In contrast, we did not observe any significant effect of Task or Task × Size interaction.

Full statistical results of all the ANOVAs are reported in Table 1. Taken together, these findings demonstrate that the earliest visual component we were able to record from the posterior cluster responded according to the physical or perceived size of the stimulus rather than its retinal size, suggesting that size-distance scaling started to occur already at ~50 ms after stimulus onset. We also provide evidence that the early stages of visual processing did not change as a function of task demands: the waveforms for manual estimation (i.e., red lines) and grasping (i.e., blue lines) overlapped one another for the entire time window.

It should be noted that similar findings were obtained using the same cluster of electrodes described in Chen et al. (2019a,b). Moreover, results of the baseline condition revealed that the ERP pattern elicited in the absence of the stimulus was completely different from the ERP pattern obtained when the disk was presented on the panel. This implies that the ERP differences depicted in Fig. 3 are not simply due to changes in viewing distance, but they rather reflect the operation of size-distance scaling in which retinal image size is combined with distance information. Results from these additional analyses are reported in Supplementary Materials.

3.1.2. ERP results from the central cluster

A 2 × 2 repeated-measures ANOVA was conducted on the peak latency and mean amplitude of the P1, N1 and P2 components of the central cluster, with Size (small vs. big) and Task (manual estimation vs. grasping) as the main factors (Fig. 4A). Full statistical results of all the ANOVAs are reported in Table 2. The analysis revealed a main effect of Size on the mean amplitude of P1 and on the peak latency of N1. In contrast with the analysis conducted on the posterior cluster, here the ANOVA revealed also a main effect of Task on the mean amplitude of P2. Interestingly, there was a significant interaction between Size and Task for the mean amplitude of the P2 component. Post-hoc pairwise comparisons with Bonferroni correction revealed significant differences between estimation small and grasping small conditions ($t_{(15)} = 7,762$, $p_{corr} < .001$) as well as between estimation big and grasping big conditions ($t_{(15)} = 5,374$, $p_{corr} < .001$). The remaining comparisons (i.e., estimation small vs. estimation big conditions and grasping small vs. grasping big conditions) did not reach significance (both $p_{corr} > .05$) (Fig. 4B). To reveal when the difference between the manual estimation and grasping became significant, we conducted point-by-point paired-sample t-tests corrected for multiple comparisons using the cluster-
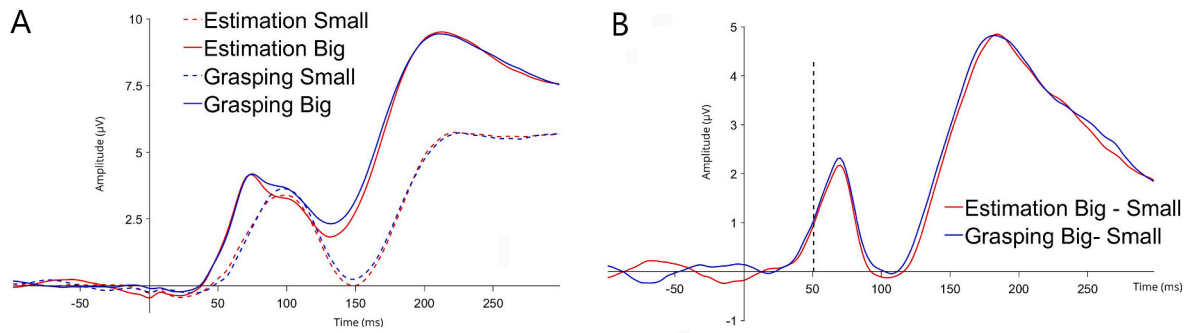
Fig. 3. A) Grand-average waveforms from the posterior cluster of six electrodes of interest (P1-Pz-P2-PO3-POZ-PO4) for each condition. Red lines indicate the condition where participants were asked to manually estimate the small or the big disk (dashed and solid lines, respectively); blue lines correspond to the condition where the participants were asked to grasp the small or the big disk (dashed and solid lines, respectively). It should be noted that the small and big disks were positioned at different viewing distances in order to subtend the same visual angle on the retina; B) Difference waveform between small and big stimulus conditions. The dashed vertical line denotes the 50% fractional area latency.

Table 1
Results of the 2 × 2 ANOVA on peak latency and mean amplitude of the P1, N1 and P2 components extracted from the posterior cluster.

	$F_{(1,15)}$	p-value	η_p^2
P1 – Peak latency			
Size	7.78	.01	.34
Task	.005	.94	<.001
Size × Task	.941	.35	.06
P1 – Mean Amplitude			
Size	9.43	<.01	.39
Task	.569	.46	.04
Size × Task	.528	.48	.03
N1 – Peak latency			
Size	36.843	<.001	.71
Task	.245	.63	.02
Size × Task	.192	.67	.01
N1 – Mean amplitude			
Size	39.343	<.001	.72
Task	3.270	.09	.18
Size × Task	1.321	.27	.08
P2 – Peak latency			
Size	9.465	<.01	.39
Task	3.784	.07	.20
Size × Task	3.499	.08	.19
P2 – Mean Amplitude			
Size	75.379	<.001	.83
Task	.001	.97	<.001
Size × Task	.114	.74	.01

Table 2
Results of the 2 × 2 ANOVA on peak latency and mean amplitude of the P1, N1 and P2 components extracted from the central cluster.

|	$F_{(1,15)}$	p-value	η_p^2
P1 – Peak latency			
Size	.093	.76	<.01
Task	.076	.79	<.01
Size × Task	1.607	.22	.10
P1 – Mean Amplitude			
Size	12.919	<.01	.46
Task	.174	.68	.01
Size × Task	.243	.63	.02
N1 – Peak latency			
Size	5.968	.03	.28
Task	2.527	.13	.14
Size × Task	.537	.47	.35
N1 – Mean amplitude			
Size	4.131	.06	.22
Task	.157	.70	.01
Size × Task	3.194	.09	.18
P2 – Peak latency			
Size	2.353	.15	.14
Task	.103	.75	<.01
Size × Task	.464	.51	.03
P2 – Mean Amplitude			
Size	.647	.43	.04
Task	50.874	<.001	.77
Size × Task	11.141	<.01	.43
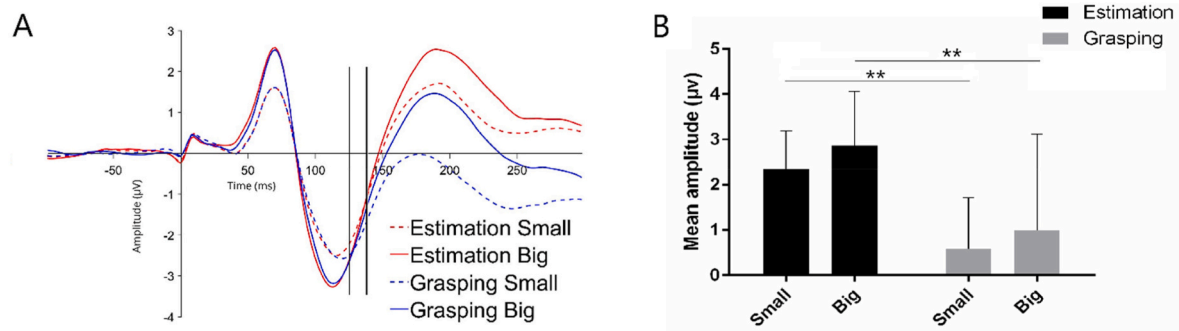
Fig. 4. A) Grand-average waveforms from the central cluster of four electrodes of interest (Cz-CP1-CPz-CP2) for each condition. Red lines indicate the condition where participants were asked to manually estimate the small or the big disk, dashed and solid lines, respectively; blue lines correspond to the condition where participants were asked to grasp the small or the big disk, dashed and solid lines, respectively. The solid thin and thick lines denote when the difference between manual estimation and grasping became significant for the small and big stimulus, respectively; B) Mean amplitude (µv) of component P2 as a function of Size and Task. Error bars represent ± 95% CIs. Asterisks (**) denote significant differences at p < .001 (Bonferroni-corrected).

based test statistic from the Fieldtrip toolbox (Oostenveld et al., 2011) (Monte Carlo method, $p_{corr} < 0.05$). The analysis revealed that the two task-related waveforms for the small stimulus overlapped until 125 ms after the stimulus onset, and then significantly separated from each other. For the big stimulus, instead, the difference between estimation and grasping waveforms became significant around 136 ms after stimulus onset (Fig. 4A). These results are in line with the outcome of ANOVA, where the main effect of the Task was detected only in correspondence to the peak of the P2 component (Fig. 4B).

Again, the ERPs reported in Fig. 4 are completely different from those observed during the baseline condition (see Fig. S1B in Supplementary Materials).

3.2. Kinematic results

Manual size estimates (MEs) and peak grip apertures (PGAs) were calculated for each condition (small and big). A 2 × 2 repeated-measures ANOVA with Size (small vs. big) and Task (manual estimation vs grasping) as main factors was carried out on MEs and PGAs. The ANOVA revealed a main effect of Size ($F_{(1,15)} = 264,385, p < .001, \eta_p^2 = 0.95$). As predicted by the principle of size constancy, participants were perfectly able to distinguish between small and big targets of constant retinal size: hand apertures were wider for the big compared to the small disks. There was also a main effect of Task ($F_{(1,15)} = 36,597, p < .001, \eta_p^2 = 0.709$): PGAs were larger than MEs. The interaction between Size and Task was also significant ($F_{(1,15)} = 15,721, p = .001, \eta_p^2 = 0.51$). Post-hoc pairwise comparisons with Bonferroni correction revealed that all the possible comparisons were significant (all $p_{corr} < .05$). The significant interaction was further explored by calculating the difference between small and big conditions separately for manual estimation and grasping (ME_big - ME_small vs. PGA_big - PGA_small). A paired-samples t-test revealed

that the difference between the small and big conditions in the manual estimation task was greater than the difference between the same conditions in the grasping task ($t_{(15)} = 3,965, p = .001$) (Fig. 5A).

We then computed the mean slopes for both manual estimation and grasping tasks. The slope values were obtained from a linear regression analysis relating hand opening and stimulus size. A slope of 1 indicates perfect size-distance scaling, whereas a shallower or steeper slope indicates less adherence to size constancy principles (Sperandio et al., 2017). As expected (Niechwiej-Szwedo et al., 2022), a paired-samples t-test revealed that the mean slope for the manual estimation task was significantly greater than the mean slope for the grasping task ($t_{(15)} = 4,017, p = .001$). It should be noted that the slope for the manual estimation task approached 1 (i.e., $M = 0.96, SD = 0.24$), demonstrating that manual estimates exhibited near-perfect size constancy (Fig. 5B).

To assess the precision of MEs and PGAs, we calculated the standard deviation for each condition. Higher variability corresponds to greater uncertainty and lower precision (Niechwiej-Szwedo et al., 2022). A 2 × 2 repeated-measures ANOVA with Size (small vs big) and Task (manual estimation vs grasping) as main factors was carried out on standard deviations. As it turned out, there was a significant effect of Size ($F_{(1,15)} = 5,833, p = .029, \eta_p^2 = 0.28$) with higher variability in response to the small target compared to the big target. The effect of Task was also significant ($F_{(1,15)} = 5,345, p = .03, \eta_p^2 = 0.26$) with higher variability during grasping compared to manual estimation. Furthermore, we found a significant interaction between Size and Task ($F_{(1,15)} = 9,696, p = .007, \eta_p^2 = 0.39$). Post-hoc pairwise comparisons with Bonferroni correction revealed significant differences between small and big conditions during manual estimation ($t_{(15)} = -3,328, p_{corr} = .02$) and grasping ($t_{(15)} = 2,873, p_{corr} < .05$). There was also a significant difference between manual estimation and grasping in the small condition ($t_{(15)} = 2,859, p_{corr} < .05$), whereas the difference between manual
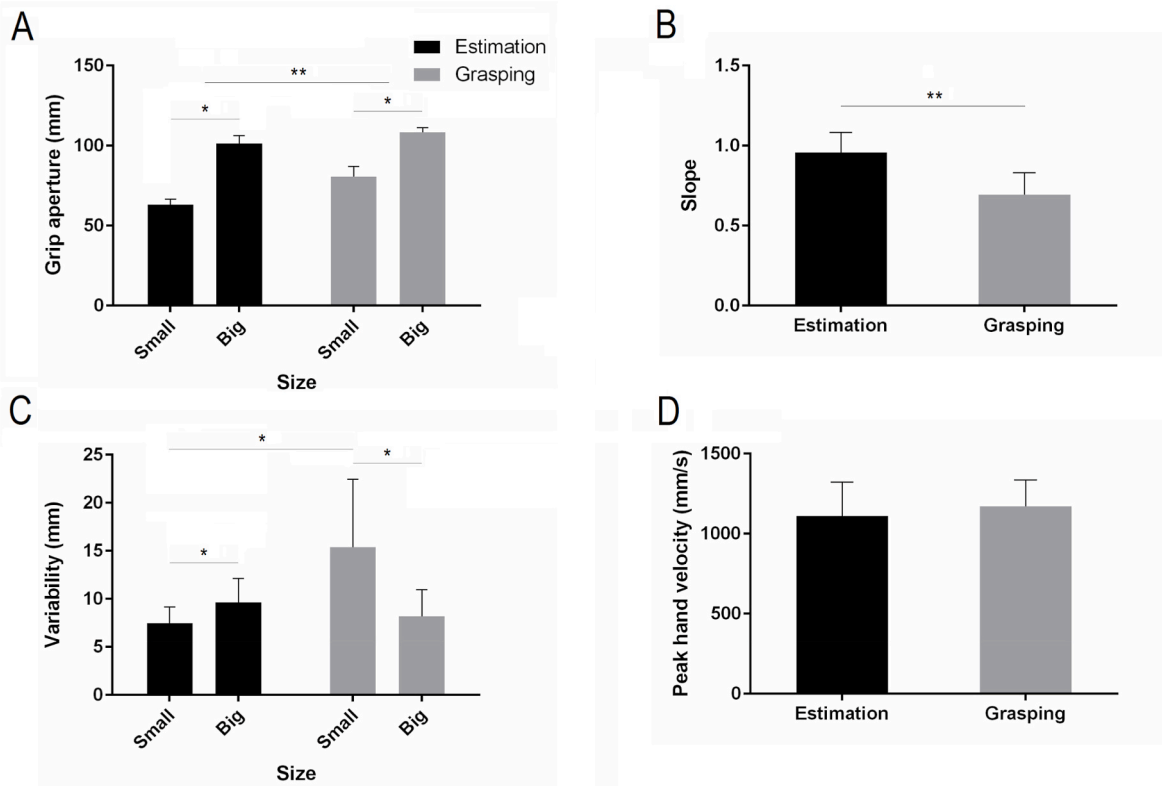

Fig. 5. Kinematic results. A) Manual estimates and peak grip apertures as a function of object size (small and big); B) Mean slope values for manual estimation and grasping tasks. Slope values were computed from a linear regression analysis relating hand opening and object size; C) Variability of manual estimates and peak grip apertures as a function of object size (small and big); D) Peak hand velocity of the reach-to-grasp movements towards the small (near) and big (far) objects. Error bars represent the 95% CI. Asterisks denote significant differences at p < .05 (*) and p < .001 (**) (Bonferroni-corrected).

estimation and grasping in the big condition was not significant ($t_{(15)} = 1,673$, $p_{corr} > .05$) (Fig. 5C). Concerning peak hand velocity (PHV), which was measured only during reach-to-grasp movements, we observed no significant difference between small (near) and big (far) objects ($t_{(15)} = -0,793$, $p = .44$). Hence, contrary to our expectations, PHV did not scale with object distance (Fig. 5D).

Finally, we carried out the same two-way ANOVA as described above on the RTs (i.e., release time) to reveal any differences across conditions in the planning phase of the movement. As it turned out, there was a main effect of Size on RTs ($F_{(1,15)} = 24,705$, $p < .001$, $\eta_p^2 = 0.62$). Release times (ms) were faster in response to the near-small ($M = 519.24$; $SD = 210.85$) compared to the far-big disks ($M = 562.35$; $SD = 236.07$). There was also a main effect of Task ($F_{(1,15)} = 13,995$, $p = .002$, $\eta_p^2 = 0.48$) with faster RTs for grasping ($M = 494.93$; $SD = 212.76$) than manual estimation ($M = 586.66$; $SD = 227.02$). However, the Size × Task interaction was not significant ($F_{(1,15)} = 3,772$, $p > .05$, $\eta_p^2 = 0.20$). Importantly, the RT analysis ensured that the time window we selected for our ERP epochs (up to 300 ms) was not contaminated by motion artifacts induced by limb movements.

3.3. Relationship between ERP and kinematic measures

To investigate if our electrophysiological data could predict individual differences in size and grip constancies, normalized values of P1, N1, and P2 amplitudes were correlated with normalized values of MEs and PGAs (i.e., 'scaling indexes', see 2.8 for additional details). The correlation revealed that there was a positive significant relationship between ME and N1 mean amplitude ($r_{(14)} = 0.49$, $p_{uncorr} < .05$) as well as between MGA and P2 mean amplitude ($r_{(14)} = 0.44$, $p_{uncorr} < .05$) of the posterior cluster (Fig. 6). None of the other correlations were significant.

4. Discussion

Previous reports have demonstrated that V1 plays a key role in size-distance integration, but seldom size constancy has been examined in real time using 3D objects and real changes in viewing distance. In the present study, we revealed the timing of the neural processes underlying size constancy for perception and action under more ecological conditions than those used so far in the literature. We presented real objects physically placed at different viewing distances, while participants had to manually estimate the perceived size of the object (perceptual task) or to reach out and grasp the target with their thumb and index finger (grasping task). Such manipulations enabled us to investigate size constancy mechanisms as they operate in the real world. Importantly, under this natural viewing paradigm, all the available monocular cues (relative size, occlusion, linear perspective, texture gradient, etc.) were completely congruent with more reliable sources of distance information derived from oculomotor adjustments, such as vergence and accommodation (Gregory, 2008; Holway and Boring, 1941; Niechwiej-Szwedo et al., 2022; Sperandio et al., 2012). In short, our findings demonstrated that stimuli that were perceived as bigger also elicited earlier and greater neural responses than those perceived as smaller. This suggests that the neural processing underlying size constancy takes place early on, at the level of P1 component peaking around 90 ms after stimulus onset. Interestingly, our findings also demonstrated that the initial stage of visual processing was independent of the purpose for which that information was used for and that task-related differences appeared only at a later point, at the level of the P2 component peaking around 200 ms after stimulus onset.

In the ensuing discussion, we will attempt to answer in detail the following questions: When does size constancy occur? Do the perception and action systems function at different time-scales? Is early visual processing shared by the two systems or does it change as a function of task demands?

4.1. Size constancy in the kinematics

As expected, kinematic results demonstrated that both manual estimations and grasp apertures were governed by size constancy: the opening of the hand scaled with the actual size of the target, even if the small and big disks had the same retinal size. These results align with previous studies showing that under full viewing conditions, when all distance cues are available, participants exhibited near-perfect size constancy in both perception and action (Chen et al., 2018; Niechwiej-Szwedo et al., 2022; Whitwell et al., 2020). Our analysis of the kinematics also revealed that grasp apertures were generally larger than manual size estimates, as typically reported in the literature (e.g., Chen et al., 2018; Niechwiej-Szwedo et al., 2022; Whitwell et al., 2020). During grasping, the hand must open much wider than the physical size of the object to avoid undesirable collisions during the reach-to-grasp movement and ensure successful contact with the target. This tendency to adopt grip apertures that exceed the edges of the object is widely interpreted as a 'safety margin' (e.g., Takemura et al., 2015; Uccelli et al., 2021). It has been argued that especially in open-loop conditions, where visual feedback of the hand or of the target object is removed, a larger safety margin of the grasping hand is required as a compensatory adjustment for uncertainty (Jakobson and Goodale, 1991; Wing et al., 1986). However, an upper limit exists for the safety margin that is dictated by the biomechanical limits of the grasping hand: obviously, the hand cannot extend wider than its anatomical dimension. As a consequence, variability in PGAs tends to decrease as object size increases, given that the possible range of safety margins is constrained by the natural limitation of the hand-opening (Utz et al., 2015). In agreement with this hypothesis, the SD associated with grasping in the present study was much reduced for the big compared to the small target. After all, our big disk was 8 cm in diameter and, thus, close to the participant's hand span, potentially leading to a 'ceiling effect'. In
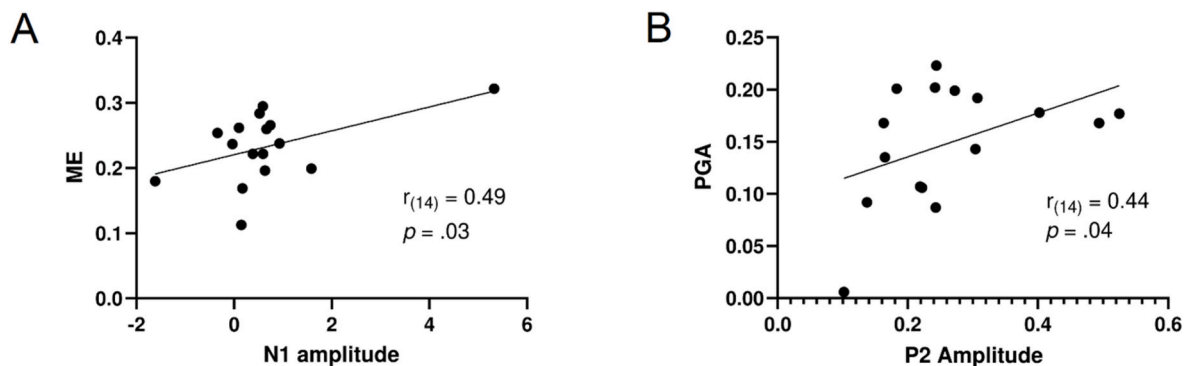

Fig. 6. A) Correlation between scaling indexes of manual size estimates and N1 amplitude; B) Correlation between scaling indexes of grasp apertures and P2 amplitude. Pearson correlation coefficients (r) and the corresponding p values (uncorrected) are reported in each panel.

contrast, manual estimation showed greater variability (i.e., SDs) for the big compared to the small stimulus conditions, as predicted by Weber's law. Weber's law is a fundamental psychophysical principle in perception, whereby our ability to detect any changes in a sensory attribute of a stimulus decreases linearly with an increase in magnitude (Fechner et al., 1966). For instance, it is relatively easy to notice a small increment in size of a small object, whereas the same amount of size increment might not be noticed for bigger objects. In other words, visual resolution decreases as object size increases. Intriguingly, Ganel and collaborators (2008a, 2008b) demonstrated, by measuring variability (SD) in perception and grasping, that unlike manual estimations which adhered to Weber's law, visually-guided actions violated this principle. This dissociation between perception and action in visual resolution has been interpreted as behavioural evidence in favor of the influential two-visual-systems hypothesis, according to which perception and action are subserved by distinct neural processes taking place in the ventral and dorsal streams, respectively (Goodale and Milner, 1992; Milner and Goodale, 2006). Our finding showing that manual estimation data obeyed Weber's law, but grasping did not, seems to agree with a wealth of evidence that goal-directed actions are immune to the effects of Weber's law (e.g., Ayala et al., 2018; Ganel et al., 2008a; Ganel et al., 2008b; Heath et al., 2011; Heath et al., 2017; Holmes and Heath, 2013). However, some cautions should be applied when interpreting the current findings. Unexpectedly, the grasping small condition generated the highest SD, whereas based on the literature cited above we would expect to see constant variability in grasp apertures regardless of object size. This increased variability indicates greater uncertainty probably due to the presence of the PDCL screen which restricted the action space between the participant's body and the near position of the movable panel. It has been shown that the predicted probability of a collision with potential obstacles affects movement duration planning and maximum grip aperture (Mon-Williams et al., 2001; Jackson et al., 1995; Tresilian, 1998). Similarly, obstacle avoidance strategies could explain why we were unable to find a significant difference in PHV between the near-small and far-big conditions, although our data showed a trend in the expected direction. In fact, previous studies have demonstrated that PHV increases progressively with target distance (Atkeson and Hollerbach, 1985; Gordon et al., 1994). In our case, higher variability was observed in the speed of the reach-to-grasp movement towards the small stimulus at near distance which affected the scaling of PHV to distance. To assess the extent to which perception and action adhered to size constancy, we calculated the slope of the linear functions relating ME and PGA to target size. We obtained a mean slope value of 0.96 for manual estimation and 0.69 for grasping. A steeper slope for manual estimation compared to grasping has been consistently reported in the literature (for a review, see Smeets and Brenner, 1999). Importantly, the slope for ME approached 1, which is indicative of perfect size-distance scaling in perception (Sperandio et al., 2017). Furthermore, we analysed RTs to reveal any differences in the preparatory phase of the movement. Participants' RTs were faster in response to the near-small than the far-big stimuli. This result contradicts previous findings where an advantage in RTs for physically (Uccelli et al., 2021) and perceptually (Sperandio et al., 2009; Sperandio, 2021) bigger objects was reported. The longer planning phase for the small target observed here could be once again explained by the increased uncertainty due to the presence of the occluding screen, which might have been interpreted by the visual system as an obstacle in the near space. Finally, participants were faster when preparing for grasping than when they had to manually estimate the disk.

To summarize, our kinematic findings confirmed that perception and action followed size constancy principles: participants were able to distinguish between small and big objects of equal retinal size. Given the interfering effects of the task-irrelevant object (PDLC screen) in the near space on different movement parameters, namely planning phase (RT), peak velocity and variability of the grasp aperture, future research should examine size and grip constancies using a set-up where the workspace is completely free from any potential obstacles.

4.2. Size constancy in the ERPs

In agreement with the kinematic results, the ERP analyses of the posterior cluster of electrodes revealed an earlier and larger neural response for the big disk compared to the small one, even though the retinal images projected by the two stimuli were always the same. Interestingly, the distinction between the small and the big stimuli, resulting from the integration between retinal image size and viewing distance information, took place significantly earlier than what was reported in a similar ERP study (Chen et al., 2019a,b). In this previous study, Chen and colleagues, by presenting images of black circles on a movable screen positioned at different distances, observed that size constancy mechanisms required about 150 ms to come into play. There are at least four possible explanations for this discrepancy in findings: firstly, there are differences in experimental settings. Chen and colleagues' (2019b) study used real manipulations of viewing distance, as we did in the current investigation. However, their visual stimuli consisted of 2D flat pictures, while we used real 3D disks. Even if the real manipulation of distance can provide reliable distance cues, 2D images have limited possibilities to return all the information conveyed by the real objects we encounter in the real world. In our study, the use of real objects might have represented a key change in unveiling the effects of size constancy at earlier visual processing stages. A growing body of evidence demonstrates that there are distinct neural mechanisms underlying the processing of 2D images and real 3D objects (Snow et al., 2011; Snow and Culham, 2021). These different neural mechanisms might enable the 'real-object advantage' reported by many behavioural studies. For example, it has been shown that real objects exert a stronger influence on attention (Gomez et al., 2018), are more easily remembered (Snow et al., 2014), break suppression faster (Korisky and Mudrik, 2021), are valued more (Bushong et al., 2010; Romero et al., 2018), and are more easily recognized by patients with visual agnosia (Chainay and Humphreys, 2001; Humphrey et al., 1994) than 2D images. Importantly, ERP studies have shown that real tools evoked stronger and more sustained action-related neural responses than their 2D counterparts (Marini et al., 2019) and that this real-world advantage in the brain response was attenuated when the real objects were positioned behind a transparent barrier (Fairchild et al., 2021), a manipulation commonly used for decreasing activation related to the potentiality for action (Caggiano et al., 2009). Overall, these findings demonstrate that real 3D objects benefit from preferential processing over 2D images. The key factor behind the real-object advantage seems to be actability or true affordance, that is the potential to physically interact with the object in a meaningful way (Snow and Culham, 2021). After all, only real objects can be acted upon and can provide haptic feedback information. This leads to our next point. Secondly, our study required participants to physically interact with the object rather than simply pressing a button. Importantly, haptic feedback was provided both in the grasping and in the manual estimation. Haptic information seems to be particularly relevant for optimizing grasping behaviours (e.g., adjusting grip aperture and force) and generating feedforward predictive models to improve performance on successive trials (Säfström and Edin, 2008). Notably, converging behavioral and fMRI evidence indicate that the neural representations underlying visuomotor control of actions directed towards real objects dissociate from those directed towards images (Freud and Ganel, 2015; Freud et al., 2018; Holmes and Heath, 2013; Hosang et al., 2016). In particular, Freud et al. (2018) have shown that activity in the left anterior intraparietal sulcus (aIPS), a dorsal brain region critical for visually-guided actions (Culham et al., 2003; Gallivan and Culham, 2015), was sensitive to real objects during the planning phase of the grasping prior to the initiation of the movement, possibly reflecting anticipation of the consequences of the interaction with the target. Thirdly, it should be noted that our stimuli were highly predictable, given that the small disk was always presented closer while the

big disk was always positioned further away from the observer's eyes. Unfortunately, we had to resort to only two object sizes to avoid excessively long EEG sessions. Although fMRI studies have shown that prediction derived from past experience can modulate the neural activity of V1 (e.g., Alink et al., 2010; Kok et al., 2012), it is still debated whether or not early stages of perceptual processing can be modulated by prior expectations. On the one hand, a number of studies have shown that predictions can affect initial perceptual processing occurring around 100–150 ms after stimulus onset (Alilović et al., 2019; Aru et al., 2016; Hsu et al., 2015; Todorovic et al., 2011; Wacongne et al., 2011), or earlier at the level of C1 component (<80 ms post-stimulus; Jabar et al., 2017), or even before stimulus onset (Kok et al., 2017; Sherman et al., 2016). On the other hand, other studies have evidenced that early sensory processing is unaltered by prior expectations and top-down modulation is observed at later stages of processing related to decision-making (Bang and Rahnev, 2017; Rao et al., 2012; Rungratsameetaweemana et al., 2018). To rule out any potential top-down effects of prediction on early visual processing, future studies should use stimuli whose size or distance cannot be easily predicted. Lastly, additional methodological differences might also explain the discrepancies among studies. For instance, the black disks used here were brighter than the black circles used in Chen et al. (2019a,b), i.e., 2.10 cd/m2 vs. 0.74 cd/m2. In addition, although the physical size of the stimuli was identical in both studies (i.e., 4 and 8 cm), the visual angle subtended by the disks in the current investigation was slightly greater than in Chen et al. (2019a,b), namely 8.8° vs 8°. This was due to the fact that the objects were positioned closer to the participants to enable them to reach the targets comfortably even at the furthest distance. Another important methodological difference concerns the baseline condition. While in the previous study, the time interval between the placement of the monitor and the onset of the stimulus varied randomly between 1.5 and 2.5 s, in the present study, the stimulus appeared right after the opening of the occluding screen and the interval between the positioning of the panel and the stimulus onset could not be temporally controlled. This limitation was due to the ecological nature of the study, which was constrained by human factors, such as the time required by the experimenter to physically position the disk on the panel and press the button to open the occluding screen. To fully disentangle these possible explanations, a direct comparison between real objects and images should be considered in a future study.

Following these observations, it can be argued that the use of 3D real objects rather than 2D images might have favored an earlier integration between retinal image size and distance cues, allowing for a faster switch from retinal size coding to perceived size coding. In the current study, we were able to detect a difference between the neural responses evoked by the two-sized stimuli within the first 100 ms post-stimulus, with the first peak of the difference waveforms recorded ~70 ms after stimulus onset. Therefore, we can conclude that size-distance scaling of real objects at real distances takes place as early as ~70 ms post-stimulus. It is difficult, however, to establish the source of this early visual component. Given that our stimuli were presented centrally, we were unable to isolate the C1 and the P1 components successfully. While it is known that the C1 component arises from V1, the generators of the P1 component have been localized in extrastriate areas (Clark et al., 1994; Di Russo et al., 2001). Moreover, the C1 component is typically characterized by an onset latency between 40 and 70 ms and a peak latency between 60 and 100 ms, whereas the P1 component starts around 65–80 ms and peaks around 100–130 ms after stimulus onset (Di Russo et al., 2001). As such, it is possible that an overlap between C1 and P1 components occurred in the present study. To better distinguish between C1 and P1 components, stimuli should be presented in the upper visual field in future studies in order to induce a negative C1 that can be easily separated from the subsequent P1 component (Clark et al., 1994).

Nonetheless, our findings are in line with previous electrophysiological studies. For example, Marg and Adams (1970) found that the receptive fields of some neurons in the occipital lobe did not respond according to retinal stimulation but followed size constancy principles when viewing distance was changed. By the same token, Ni et al. (2014) found that the activity of a number of neurons in monkey V1 reflected illusory size perception generated by a Ponzo background, instead of the retinal size of the stimuli, as a result of shifts in the position of the receptive fields. Interestingly, the shifts occurred remarkably early, starting from 30 ms after stimulus presentation. More recently, Chen and colleagues (Chen et al., 2019a,b), have shown by recording steady-state visually evoked potentials (SSVEP), which are known to originate in the early visual cortex, that about 50% of size-distance scaling occurred in V1. Our findings are further supported by the evidence that space-related information (e.g., distance cues, vergence, retinal disparity, gaze direction) can modulate neural activity already from the earliest processing stages (Weyand and Malpeli, 1993; Masson et al., 1997; Dobbins et al., 1998; Trotter and Celebrini, 1999; Trotter et al., 1992, 2004). Previous fMRI studies reporting patterns of activity in V1 compatible with perceived size (Fang et al., 2008; Murray et al., 2006; Pooresmaeili et al., 2013; Schwarzkopf et al., 2011; Schwarzkopf and Rees, 2013; Sperandio et al., 2012; Weidner et al., 2014) are also consistent with the idea that size constancy plays out in the neural response of V1. The fact that size constancy was present in the initial part of the visual ERP response does not exclude the role of top-down influences from high-order visual areas on feedforward sensory processing in V1 (e.g., Di Russo et al., 2001; Gomez Gonzalez et al., 1994). Our findings are also consistent with the hypothesis of rapid feedback connections, possibly carrying distance information processed at later stages, which can exert modulations on the early visual response in V1 (Hupé et al., 2001; Girard et al., 2001).

To reveal any task-related differences in the ERPs, we carried out an additional analysis on a cluster of central electrodes which was identified by comparing the neural activity elicited by the estimation and the grasping tasks. This analysis revealed an earlier effect of object size on the first positive and the first negative ERP components, with the big stimulus eliciting a larger and faster neural response than the small stimulus, similar to what we obtained from the posterior electrodes. However, the most interesting result here was related to the P2 component: we observed a greater amplitude for manual estimation than grasping. As shown by the cluster-based permutation analysis, the difference between the tasks began earlier for the small stimulus condition than the big stimulus condition. It has been argued that the N1 component reflects reactivation of the extrastriate visual area V3A, while the P2 component reflects reactivation of occipital visual areas including V1 as a result of top-down feedback from higher-level visual areas (Di Russo et al., 2008). Moreover, an ERP study on the Ponzo illusion demonstrated that the amplitude of the P2 component changed as a function of perceived size, suggesting that the integration of retinal image size and pictorial depth cues conveyed by the illusory background occurred at later stages of visual processing as a result of top-down modulation (Liu et al., 2009). Therefore, we speculate that manual estimation might have involved greater feedback from higher-level visual areas than grasping in computing perceived size.

4.3. Correlations between grip apertures and visual processing emerge in the later ERP components

Finally, the correlations between 'scaling indexes' of electrophysiological and the kinematic data revealed a moderate positive association between the mean amplitude of the first negative-going ERP component (N1) and the mean grip aperture registered during manual estimation. Grasping, instead, was characterized by a moderate positive association between the mean amplitude of the second positive-going ERP component (P2) and the peak grip aperture (PGA) of the hand. These findings are novel and suggest a link between individual differences in size constancy in perception and action and later stages of visual processing. Based on the literature, the modulation of N1 amplitude is frequently associated with tasks requiring attention and cognitive efforts (Callaway

and Halliday, 1982; Hillyard and Anllo-Vento, 1998; Weisz and Schlittmeier, 2006). We hypothesize that the correlation between the N1 amplitude and manual estimation could be due to the efforts and the attention necessary to make accurate judgments of object size in a less automatic way than when participants were required to grasp the target. Surprisingly, we also obtained a significant correlation between PGA and the P2 component, which would suggest re-activation of V1 and other extrastriate visual areas (Di Russo et al., 2008). Previous studies have shown that there are instances in which the dorsal stream is required to interact with the ventral stream in order to perform successful actions (Singhal et al., 2013; Westwood et al., 2000; Westwood and Goodale, 2003). It should be noted that in our case grasping was performed in an open-loop condition and participants might have adopted strategies to avoid collision with the occlusion screen as they reached to grasp the disks (see section 4.1 for further discussion). This might have determined the relationship between grasp apertures and the P2 component. Nonetheless, our findings demonstrate that the neural coding of grip constancy was already present at the earliest cortical stages during the planning phase of the reach-to-grasp movement, thus suggesting rapid size-distance integration in processing grasp aperture.

5. Conclusion

Taken together, the results obtained from the present study raise the possibility of an early visual locus for size constancy in perception and action. Interestingly, neural processing at the earliest cortical stages was unaffected by task demands. Task-related effects, instead, were only observed later and possibly reflected greater top-down modulations in manual size estimation. These results converge with findings from multiple lines of research using different methodological approaches and corroborate the hypothesis that size-constancy operations take place already at the level of V1. Future research should bring new information about the origins of this size-distance integration, using techniques that can provide both high spatial and temporal resolution.

CRediT authorship contribution statement

Simona Noviello: Data curation, Formal analysis, Investigation, Methodology, Project administration, Software, Writing - original draft, Writing - review & editing. **Saman Kamari Songhorabadi:** Data curation, Formal analysis, Investigation, Methodology, Project administration, Writing - review & editing. **Zhiqing Deng:** Formal analysis, Software. **Chao Zheng:** Formal analysis, Software. **Juan Chen:** Conceptualization, Methodology, Writing - review & editing, Supervision. **Angelo Pisani:** Data curation, Formal analysis. **Elena Franchin:** Data curation, Formal analysis, Investigation. **Enrica Pierotti:** Methodology, Software. **Elena Tonolli:** Methodology. **Simona Monaco:** Resources. **Louis Renoult:** Funding acquisition, Supervision, Writing - review & editing. **Irene Sperandio:** Conceptualization, Data curation, Funding acquisition, Methodology, Supervision, Writing - original draft, Writing - review & editing.

Data availability

Data will be made available on request.

Acknowledgments

Appendix A. Supplementary data

Supplementary data to this article can be found online at https://doi.org/10.1016/j.neuropsychologia.2023.108746.

References

Alilović, J., Timmermans, B., Reteig, L.C., van Gaal, S., Slagter, H.A., 2019. No evidence that predictions and attention modulate the first feedforward sweep of cortical information processing. Cerebr. Cortex 29 (5), 2261–2278. https://doi.org/10.1093/cercor/bhz038.

Alink, A., Schwiedrzik, C.M., Kohler, A., Singer, W., Muckli, L., 2010. Stimulus predictability reduces responses in primary visual cortex. J. Neurosci.: The Official Journal of the Society for Neuroscience 30 (8), 2960–2966. https://doi.org/10.1523/JNEUROSCI.3730-10.2010.

Aru, J., Rutiku, R., Wibral, M., Singer, W., Melloni, L., 2016. Early Effects of Previous Experience on Conscious Perception. Neuroscience of Consciousness. https://doi.org/10.1093/nc/niw004 niw004.

Atkeson, C.G., Hollerbach, J.M., 1985. Kinematic features of unrestrained vertical arm movements. J. Neurosci. 5 (9), 2318–2330. https://doi.org/10.1523/JNEUROSCI.05-09-02318.1985.

Ayala, N., Binsted, G., Heath, M., 2018. Hand anthropometry and the limits of aperture separation determine the utility of Weber's law in grasping and manual estimation. Exp. Brain Res. 236 (8), 2439–2446. https://doi.org/10.1007/s00221-018-5311-6.

Bang, J.W., Rahnev, D., 2017. Stimulus expectation alters decision criterion but not sensory signal in perceptual decision making. Sci. Rep. 7 (1), 1. https://doi.org/10.1038/s41598-017-16885-2.

Bell, A.J., Sejnowski, T.J., 1995. An information-maximization approach to blind separation and blind deconvolution. Neural Comput. 7 (6), 1129–1159. https://doi.org/10.1162/neco.1995.7.6.1129.

Brainard, D.H., 1997. The psychophysics toolbox. Spatial Vis. 10 (4), 433–436. https://doi.org/10.1163/156856897X00357.

Bushong, B., King, L.M., Camerer, C.F., Rangel, A., 2010. Pavlovian processes in consumer choice: the physical presence of a good increases willingness-to-pay. Am. Econ. Rev. 100 (4), 1556–1571. https://doi.org/10.1257/aer.100.4.1556.

Caggiano, V., Fogassi, L., Rizzolatti, G., Thier, P., Casile, A., 2009. Mirror neurons differentially encode the peripersonal and extrapersonal space of monkeys. Science (New York, N.Y.) 324 (5925), 403–406. https://doi.org/10.1126/science.1166818.

Callaway, E., Halliday, R., 1982. The effect of attentional effort on visual evoked potential N1 latency. Psychiatr. Res. 7 (3), 299–308. https://doi.org/10.1016/0165-1781(82)90066-X.

Chainay, H., Humphreys, G.W., 2001. The real-object advantage in agnosia: evidence for a role of surface and depth information in object recognition. Cogn. Neuropsychol. 18 (2), 175–191. https://doi.org/10.1080/02643290042000062.

Chen, Jing, McManus, M., Valsecchi, M., Harris, L.R., Gegenfurtner, K.R., 2019a. Steady-state visually evoked potentials reveal partial size constancy in early visual cortex. J. Vis. 19 (6), 8. https://doi.org/10.1167/19.6.8.

Chen, J., Sperandio, I., Goodale, M.A., 2018. Proprioceptive distance cues restore perfect size constancy in grasping, but not perception, when vision is limited. Curr. Biol. 28 (6), 927–932.e4. https://doi.org/10.1016/j.cub.2018.01.076.

Chen, J., Sperandio, I., Henry, M.J., Goodale, M.A., 2019b. Changing the real viewing distance reveals the temporal evolution of size constancy in visual cortex. Curr. Biol. 29 (13), 2237–2243.e4. https://doi.org/10.1016/j.cub.2019.05.069.

Chouinard, P.A., Noulty, W.A., Sperandio, I., Landry, O., 2013. Global processing during the Müller-Lyer illusion is distinctively affected by the degree of autistic traits in the typical population. Exp. Brain Res. 230 (2), 219–231. https://doi.org/10.1007/s00221-013-3646-6.

Chouinard, P.A., Unwin, K.L., Landry, O., Sperandio, I., 2016. Susceptibility to optical illusions varies as a function of the autism-spectrum quotient but not in ways predicted by local-global biases. J. Autism Dev. Disord. 46 (6), 2224–2239. https://doi.org/10.1007/s10803-016-2753-1.

Clark, V.P., Fan, S., Hillyard, S.A., 1994. Identification of early visual evoked potential generators by retinotopic and topographic analyses. Hum. Brain Mapp. 2 (3), 170–187. https://doi.org/10.1002/hbm.460020306.

Culham, J.C., Danckert, S.L., DeSouza, J.F.X., Gati, J.S., Menon, R.S., Goodale, M.A., 2003. Visually guided grasping produces fMRI activation in dorsal but not ventral stream brain areas. Exp. Brain Res. 153 (2), 180–189. https://doi.org/10.1007/s00221-003-1591-5.

Delorme, A., Makeig, S., 2004. EEGLAB: an open source toolbox for analysis of single-trial EEG dynamics including independent component analysis. J. Neurosci. Methods 134 (1), 9–21. https://doi.org/10.1016/j.jneumeth.2003.10.009lopez.

Di Russo, F., Aprile, T., Spitoni, G., Spinelli, D., 2008. Impaired visual processing of contralesional stimuli in neglect patients: a visual-evoked potential study. Brain: J. Neurol. 131 (Pt 3), 842–854. https://doi.org/10.1093/brain/awm281.

Di Russo, F., Martínez, A., Sereno, M.I., Pitzalis, S., Hillyard, S.A., 2001. Cortical sources of the early components of the visual evoked potential. Hum. Brain Mapp. 15, 95–111. https://doi.org/10.1002/hbm.10010.

Dobbins, A.C., Jeo, R.M., Fiser, J., Allman, J.M., 1998. Distance modulation of neural activity in the visual cortex. Science 281 (5376), 552–555. https://doi.org/10.1126/science.281.5376.552.

Fairchild, G.T., Marini, F., Snow, J.C., 2021. Graspability modulates the stronger neural signature of motor preparation for real objects vs. Pictures. J. Cognit. Neurosci. 33 (12), 2477–2493. https://doi.org/10.1162/jocn_a_01771.

Fang, F., Boyaci, H., Kersten, D., Murray, S.O., 2008. Attention-dependent representation of a size illusion in human V1. Curr. Biol. 18 (21), 1707–1712. https://doi.org/10.1016/j.cub.2008.09.025.

Fechner, G.T., Adler, H.E., Howes, D.H., Boring, E.G., 1966. Elements of Psychophysics. Holt, Rinehart and Winston.

Freud, E., Ganel, T., 2015. Visual control of action directed toward two-dimensional objects relies on holistic processing of object shape. Psychonomic Bull. Rev. 22 (5), 1377–1382. https://doi.org/10.3758/s13423-015-0803-x.

Freud, E., Macdonald, S.N., Chen, J., Quinlan, D.J., Goodale, M.A., Culham, J.C., 2018. Getting a grip on reality: grasping movements directed to real objects and images rely on dissociable neural representations. Cortex; a J. Devot. Study Nervous Syst. Behav. 98, 34–48. https://doi.org/10.1016/j.cortex.2017.02.020.

Gallivan, J.P., Culham, J.C., 2015. Neural coding within human brain areas involved in actions. Curr. Opin. Neurobiol. 33, 141–149. https://doi.org/10.1016/j.conb.2015.03.012.

Ganel, T., Chajut, E., Algom, D., 2008a. Visual coding for action violates fundamental psychophysical principles. Curr. Biol. 18 (14), R599–R601. https://doi.org/10.1016/j.cub.2008.04.052.

Ganel, T., Chajut, E., Tanzer, M., Algom, D., 2008b. Response: when does grasping escape Weber's law? Curr. Biol. 18 (23), R1090–R1091. https://doi.org/10.1016/j.cub.2008.10.007.

Girard, P., Hupé, J.M., Bullier, J., 2001. Feedforward and feedback connections between areas V1 and V2 of the monkey have similar rapid conduction velocities. J. Neurophysiol. 85 (3), 1328–1331. https://doi.org/10.1152/jn.2001.85.3.1328.

Glickstein, M., Whitteridge, D., 1987. Tatsuji Inouye and the mapping of the visual fields on the human cerebral cortex. Trends Neurosci. 10 (9), 350–353. https://doi.org/10.1016/0166-2236(87)90066-X.

Gomez Gonzalez, C.M., Clark, V.P., Fan, S., Luck, S.J., Hillyard, S.A., 1994. Sources of attention-sensitive visual event-related potentials. Brain Topogr. 7, 41–51. https://doi:10.1007/BF01184836.

Gomez, M.A., Skiba, R.M., Snow, J.C., 2018. Graspable objects grab attention more than images do. Psychol. Sci. 29 (2), 206–218. https://doi.org/10.1177/0956797617730599.

Goodale, M.A., Milner, A.D., 1992. Separate visual pathways for perception and action. Trends Neurosci. 15 (1), 20–25. https://doi.org/10.1016/0166-2236(92)90344-8.

Gordon, J., Ghilardi, M.F., Ghez, C., 1994. Accuracy of planar reaching movements. Exp. Brain Res. 99 (1), 97–111. https://doi.org/10.1007/BF00241415.

Gregory, R.L., 2008. Emmert's Law and the moon illusion. Spatial Vis. 21 (3–5), 407–420. https://doi.org/10.1163/156856808784532509.

Heath, M., Manzone, J., Khan, M., Davarpanah Jazi, S., 2017. Vision for action and perception elicit dissociable adherence to Weber's law across a range of «graspable» target objects. Exp. Brain Res. 235 (10), 3003–3012. https://doi.org/10.1007/s00221-017-5025-1.

Heath, M., Mulla, A., Holmes, S.A., Smuskowitz, L.R., 2011. The visual coding of grip aperture shows an early but not late adherence to Weber's law. Neurosci. Lett. 490 (3), 200–204. https://doi.org/10.1016/j.neulet.2010.12.051.

Hillyard, S.A., Anllo-Vento, L., 1998. Event-related brain potentials in the study of visual selective attention. Proc. Natl. Acad. Sci. U.S.A. 95 (3), 781–787. https://doi.org/10.1073/pnas.95.3.781.

Holmes, G., 1918. Disturbances of vision by cerebral lesions. Br. J. Ophthalmol. 2 (7), 353–384. https://doi.org/10.1136/bjo.2.7.353.

Holmes, S.A., Heath, M., 2013. Goal-directed grasping: the dimensional properties of an object influence the nature of the visual information mediating aperture shaping. Brain Cognit. 82 (1), 18–24. https://doi.org/10.1016/j.bandc.2013.02.005.

Holway, A.H., Boring, E.G., 1941. Determinants of apparent visual size with distance variant. Am. J. Psychol. 54 (1), 21–37. https://doi.org/10.2307/1417790.

Hosang, S., Chan, J., Davarpanah Jazi, S., Heath, M., 2016. Grasping a 2D object: terminal haptic feedback supports an absolute visuo-haptic calibration. Exp. Brain Res. 234 (4), 945–954. https://doi.org/10.1007/s00221-015-4521-4.

Hsu, Y.-F., Bars, S.L., Hämäläinen, J.A., Waszak, F., 2015. Distinctive representation of mispredicted and unpredicted prediction errors in human electroencephalography. J. Neurosci. 35 (43), 14653–14660. https://doi.org/10.1523/JNEUROSCI.2204-15.2015.

Hu, Y., Eagleson, R., Goodale, M.A., 1999. The effects of delay on the kinematics of grasping. Exp. Brain Res. 126 (1), 109–116. https://doi.org/10.1007/s002210050720.

Hu, Y., Goodale, M.A., 2000. Grasping after a delay shifts size-scaling from absolute to relative metrics. J. Cognit. Neurosci. 12 (5), 856–868. https://doi.org/10.1162/089892900562462.

Humphrey, G.K., Goodale, M.A., Jakobson, L.S., Servos, P., 1994. The role of surface information in object recognition: studies of a visual form agnosic and normal subjects. Perception 23 (12), 1457–1481. https://doi.org/10.1068/p231457.

Hupé, J.M., James, A.C., Girard, P., Lomber, S.G., Payne, B.R., Bullier, J., 2001. Feedback connections act on the early part of the responses in monkey visual cortex. J. Neurophysiol. 85 (1), 134–145. https://doi.org/10.1152/jn.2001.85.1.134.

Jabar, S.B., Filipowicz, A., Anderson, B., 2017. Tuned by experience: how orientation probability modulates early perceptual processing. Vis. Res. 138, 86–96. https://doi.org/10.1016/j.visres.2017.07.008.

Jackson, S.R., Jackson, G.M., Rosicky, J., 1995. Are non-relevant objects represented in working memory? The effect of non-target objects on reach and grasp kinematics. Exp. Brain Res. 102 (3), 519–530. https://doi.org/10.1007/BF00230656.

Jakobson, L.S., Goodale, M.A., 1991. Factors affecting higher-order movement planning: a kinematic analysis of human prehension. Exp. Brain Res. 86 (1), 199–208. https://doi.org/10.1007/BF00231054.

Jeannerod, M., 1984. The timing of natural prehension movements. J. Mot. Behav. 16 (3), 235–254. https://doi.org/10.1080/00222895.1984.10735319.

Kiesel, A., Miller, J., Jolicoeur, P., Brisson, B., 2008. Measurement of ERP latency differences: a comparison of single-participant and jackknife-based scoring methods. Psychophysiology 45 (2), 250–274. https://doi.org/10.1111/j.1469-8986.2007.00618.x.

Kleiner, M., Brainard, D., Pelli, D., Ingling, A., Murray, R., Broussard, C., 2007. What's new in psychtoolbox-3. Perception 36 (14), 1–16. https://doi.org/10.1068/v070821.

Kok, P., Jehee, J.F.M., de Lange, F.P., 2012. Less is more: expectation sharpens representations in the primary visual cortex. Neuron 75 (2), 265–270. https://doi.org/10.1016/j.neuron.2012.04.034.

Kok, P., Mostert, P., de Lange, F.P., 2017. Prior expectations induce prestimulus sensory templates. Proc. Natl. Acad. Sci. USA 114 (39), 10473–10478. https://doi.org/10.1073/pnas.1705652114.

Korisky, U., Mudrik, L., 2021. Dimensions of perception: 3D real-life objects are more readily detected than their 2D images. Psychol. Sci. 32 (10), 1636–1648. https://doi.org/10.1177/09567976211010718.

Kudoh, N., Hattori, M., Numata, N., Maruyama, K., 1997. An analysis of spatiotemporal variability during prehension movements: effects of object size and distance. Exp. Brain Res. 117 (3), 457–464. https://doi.org/10.1007/s002210050241.

Liu, Q., Wu, Y., Yang, Q., Campos, J.L., Zhang, Q., Sun, H.-J., 2009. Neural correlates of size illusions: an event-related potential study. Neuroreport 20 (8), 809–814. https://doi.org/10.1097/WNR.0b013e32832be7c0.

Lopez-Calderon, J., Luck, S.J., 2014. ERPLAB: an open-source toolbox for the analysis of event-related potentials. Front. Hum. Neurosci. 8. https://www.frontiersin.org/articles/10.3389/fnhum.2014.00213.

Marg, E., Adams, J.E., 1970. Evidence for a neurological zoom system in vision from angular changes in some receptive fields of single neurons with changes in fixation distance in the human visual cortex. Experientia 26 (3), 270–271. https://doi.org/10.1007/BF01900088.

Marini, F., Breeding, K.A., Snow, J.C., 2019. Distinct visuo-motor brain dynamics for real-world objects versus planar images. Neuroimage 195, 232–242. https://doi.org/10.1016/j.neuroimage.2019.02.026.

Marotta, J.J., Behrmann, M., Goodale, M.A., 1997. The removal of binocular cues disrupts the calibration chenof grasping in patients with visual form agnosia. Exp. Brain Res. 116 (1), 113–121. https://doi.org/10.1007/PL00005731.

Masson, G.S., Busettini, C., Miles, F.A., 1997. Vergence eye movements in response to binocular disparity without depth perception. Nature 389 (6648), 6648. https://doi.org/10.1038/38496.

Milner, D., Goodale, M., 2006. The Visual Brain in Action. OUP Oxford. https://doi.org/10.1093/acprof:oso/9780198524724.001.0001.

Mon-Williams, M., Tresilian, J.R., Coppard, V.L., Carson, R.G., 2001. The effect of obstacle position on reach-to-grasp movements. Exp. Brain Res. 137 (3), 497–501. https://doi.org/10.1007/s002210100684.

Murray, S.O., Boyaci, H., Kersten, D., 2006. The representation of perceived angular size in human primary visual cortex. Nat. Neurosci. 9 (3), 3. https://doi.org/10.1038/nn1641.

Ni, A.M., Murray, S.O., Horwitz, G.D., 2014. Object-centered shifts of receptive field positions in monkey primary visual cortex. Curr. Biol. 24 (14), 1653–1658. https://doi.org/10.1016/j.cub.2014.06.003.

Niechwiej-Szwedo, E., Cao, M., Barnett-Cowan, M., 2022. Binocular viewing facilitates size constancy for grasping and manual estimation. Vision 6 (2), 2. https://doi.org/10.3390/vision6020023.

Oldfield, R.C., 1971. The assessment and analysis of handedness: the Edinburgh inventory. Neuropsychologia 9 (1), 97–113. https://doi.org/10.1016/0028-3932(71)90067-4.

Oostenveld, R., Fries, P., Maris, E., Schoffelen, J.-M., 2011. FieldTrip: open source software for advanced analysis of MEG, EEG, and invasive electrophysiological data. Comput. Intell. Neurosci. 2011, 1–9. https://doi.org/10.1155/2011/156869, 1-1.

Pelli, D.G., 1997. The VideoToolbox software for visual psychophysics: transforming numbers into movies. Spatial Vis. 10 (4), 437–442. https://doi.org/10.1163/156856897X00366.

Pion-Tonachini, L., Kreutz-Delgado, K., Makeig, S., 2019. ICLabel: an automated electroencephalographic independent component classifier, dataset, and website. Neuroimage 198, 181–197. https://doi.org/10.1016/j.neuroimage.2019.05.026.

Pooresmaeili, A., Arrighi, R., Biagi, L., Morrone, M.C., 2013. Blood oxygen level-dependent activation of the primary visual cortex predicts size adaptation illusion. J. Neurosci. 33 (40), 15999–16008. https://doi.org/10.1523/JNEUROSCI.1770-13.2013.

Rao, V., DeAngelis, G.C., Snyder, L.H., 2012. Neural correlates of prior expectations of motion in the lateral intraparietal and middle temporal areas. J. Neurosci.: The Official Journal of the Society for Neuroscience 32 (29), 10063–10074. https://doi.org/10.1523/JNEUROSCI.5948-11.2012.

Romero, C.A., Compton, M.T., Yang, Y., Snow, J.C., 2018. The real deal: willingness-to-pay and satiety expectations are greater for real foods versus their images. Cortex; a J. Devot. Study Nervous Syst. Behav. 107, 78–91. https://doi.org/10.1016/j.cortex.2017.11.010.

Rosner, B., 1975. On the detection of many outliers. Technometrics 17 (2), 221–227. https://doi.org/10.2307/1268354.

Rungratsameetaweemana, N., Itthipuripat, S., Salazar, A., Serences, J.T., 2018. Expectations do not alter early sensory processing during perceptual decision-

making. J. Neurosci. 38 (24), 5632–5648. https://doi.org/10.1523/JNEUROSCI.3638-17.2018.

Säfström, D., Edin, B.B., 2008. Prediction of object contact during grasping. Exp. Brain Res. 190 (3), 265–277. https://doi.org/10.1007/s00221-008-1469-7.

Schwarzkopf, D.S., Rees, G., 2013. Subjective size perception depends on central visual cortical magnification in human V1. PLoS One 8 (3), e60550. https://doi.org/10.1371/journal.pone.0060550.

Schwarzkopf, D.S., Song, C., Rees, G., 2011. The surface area of human V1 predicts the subjective experience of object size. Nat. Neurosci. 14 (1), 28–30. https://doi.org/10.1038/nn.2706.

Servos, P., Goodale, M.A., Jakobson, L.S., 1992. The role of binocular vision in prehension: a kinematic analysis. Vis. Res. 32 (8), 1513–1521. https://doi.org/10.1016/0042-6989(92)90207-Y.

Sherman, M.T., Kanai, R., Seth, A.K., VanRullen, R., 2016. Rhythmic influence of top-down perceptual priors in the phase of prestimulus occipital alpha oscillations. J. Cognit. Neurosci. 28 (9), 1318–1330. https://doi.org/10.1162/jocn_a_00973.

Singhal, A., Monaco, S., Kaufman, L.D., Culham, J.C., 2013. Human fMRI reveals that delayed action Re-recruits visual perception. PLoS One 8 (9), e73629. https://doi.org/10.1371/journal.pone.0073629.

Smeets, J.B.J., Brenner, E., 1999. A new view on grasping. Mot. Control 3 (3), 237–271. https://doi.org/10.1123/mcj.3.3.237.

Smith, J.D., Marg, E., 1975. Zoom neurons in visual cortex: receptive field enlargements with near fixation in monkeys. Experientia 31 (3), 323–326. https://doi.org/10.1007/BF01922564.

Snow, J.C., Culham, J.C., 2021. The treachery of images: how realism influences brain and behavior. Trends Cognit. Sci. 25 (6), 506–519. https://doi.org/10.1016/j.tics.2021.02.008.

Snow, J.C., Pettypiece, C.E., McAdam, T.D., McLean, A.D., Stroman, P.W., Goodale, M. A., Culham, J.C., 2011. Bringing the real world into the fMRI scanner: repetition effects for pictures versus real objects. Sci. Rep. 1 (1) https://doi.org/10.1038/srep00130. Art. 1.

Snow, J.C., Skiba, R.M., Coleman, T.L., Berryhill, M.E., 2014. Real-world objects are more memorable than photographs of objects. Front. Hum. Neurosci. 8, 837. https://doi.org/10.3389/fnhum.2014.00837.

Sperandio, I., 2021. Developmental trajectories of size constancy as implicitly examined by simple reaction times. Vision 5 (4). https://doi.org/10.3390/vision5040050. Art. 4.

Sperandio, I., Chouinard, P.A., 2015. The mechanisms of size constancy. Multisensory Res. 28 (3–4), 253–283. https://doi.org/10.1163/22134808-00002483.

Sperandio, I., Chouinard, P.A., Goodale, M.A., 2012. Retinotopic activity in V1 reflects the perceived and not the retinal size of an afterimage. Nat. Neurosci. 15 (4), 4. https://doi.org/10.1038/nn.3069.

Sperandio, I., Kaderali, S., Chouinard, P.A., Frey, J., Goodale, M.A., 2013. Perceived size change induced by nonvisual signals in darkness: the relative contribution of vergence and proprioception. J. Neurosci. 33 (43), 16915–16923. https://doi.org/10.1523/JNEUROSCI.0977-13.2013.

Sperandio, I., Savazzi, S., Gregory, R.L., Marzi, C.A., 2009. Visual reaction time and size constancy. Perception 38 (11), 1601–1609. https://doi.org/10.1068/p6421.

Sperandio, I., Unwin, K.L., Landry, O., Chouinard, P.A., 2017. Size constancy is preserved but afterimages are prolonged in typical individuals with higher degrees of self-reported autistic traits. J. Autism Dev. Disord. 47 (2), 447–459. https://doi.org/10.1003-016-2971-6.

Stone, J.V., 2002. Independent component analysis: an introduction. Trends Cognit. Sci. 6 (2), 59–64. https://doi.org/10.1016/S1364-6613(00)01813-1.

Takemura, N., Fukui, T., Inui, T., 2015. A computational model for aperture control in reach-to-grasp movement based on predictive variability. Front. Comput. Neurosci. 9 https://doi.org/10.3389/fncom.2015.00143.

Todorovic, A., van Ede, F., Maris, E., de Lange, F.P., 2011. Prior expectation mediates neural adaptation to repeated sounds in the auditory cortex: an MEG study. J. Neurosci.: The Official Journal of the Society for Neuroscience 31 (25), 9118–9123. https://doi.org/10.1523/JNEUROSCI.1425-11.2011.

Tootell, R.B., Silverman, M.S., Switkes, E., De Valois, R.L., 1982. Deoxyglucose analysis of retinotopic organization in primate striate cortex. Science (New York, N.Y.) 218 (4575), 902–904. https://doi.org/10.1126/science.7134981.

Tresilian, J.R., 1998. Attention in action or obstruction of movement? A kinematic analysis of avoidance behavior in prehension. Exp. Brain Res. 120 (3), 352–368. https://doi.org/10.1007/s002210050409.

Trotter, Y., Celebrini, S., 1999. Gaze direction controls response gain in primary visual-cortex neurons. Nature 398 (6724), 6724. https://doi.org/10.1038/18444.

Trotter, Y., Celebrini, S., Durand, J.B., 2004. Evidence for implication of primate area V1 in neural 3-D spatial localization processing. J. Physiol. Paris 98 (1), 125–134. https://doi.org/10.1016/j.jphysparis.2004.03.004.

Trotter, Y., Celebrini, S., Stricanne, B., Thorpe, S., Imbert, M., 1992. Modulation of neural stereoscopic processing in primate area V1 by the viewing distance. Science 257 (5074), 1279–1281. https://doi.org/10.1126/science.1519066.

Uccelli, S., Pisu, V., Bruno, N., 2021. Precision in grasping: consistent with Weber's law, but constrained by "safety margins". Neuropsychologia 163, 108088. https://doi.org/10.1016/j.neuropsychologia.2021.108088.

Utz, K.S., Hesse, C., Aschenneller, N., Schenk, T., 2015. Biomechanical factors may explain why grasping violates Weber's law. Vis. Res. 111, 22–30. https://doi.org/10.1016/j.visres.2015.03.021.

Wacongne, C., Labyt, E., van Wassenhove, V., Bekinschtein, T., Naccache, L., Dehaene, S., 2011. Evidence for a hierarchy of predictions and prediction errors in human cortex. Proc. Natl. Acad. Sci. USA 108 (51), 20754–20759. https://doi.org/10.1073/pnas.1117807108.

Weidner, R., Plewan, T., Chen, Q., Buchner, A., Weiss, P.H., Fink, G.R., 2014. The moon illusion and size-distance scaling—evidence for shared neural patterns. J. Cognit. Neurosci. 26 (8), 1871–1882. https://doi.org/10.1162/jocn_a_00590.

Weisz, N., Schlittmeier, S.J., 2006. Detrimental effects of irrelevant speech on serial recall of visual items are reflected in reduced visual N1 and reduced theta activity. Cerebr. Cortex 16 (8), 1097–1105. https://doi.org/10.1093/cercor/bhj051.

Westwood, D.A., Goodale, M.A., 2003. Perceptual illusion and the real-time control of action. Spatial Vis. 16 (3–4), 243–254. https://doi.org/10.1163/156856803322467518.

Westwood, D.A., Heath, M., Roy, E.A., 2000. The effect of a pictorial illusion on closed-loop and open-loop prehension. Exp. Brain Res. 134 (4), 456–463. https://doi.org/10.1007/s002210000489.

Weyand, T.G., Malpeli, J.G., 1993. Responses of neurons in primary visual cortex are modulated by eye position. J. Neurophysiol. 69 (6), 2258–2260. https://doi.org/10.1152/jn.1993.69.6.2258.

Whitwell, R.L., Sperandio, I., Buckingham, G., Chouinard, P.A., Goodale, M.A., 2020. Grip constancy but not perceptual size constancy survives lesions of early visual cortex. Curr. Biol. 30 (18), 3680–3686.e5. https://doi.org/10.1016/j.cub.2020.07.026.

Wing, A.M., Turton, A., Fraser, C., 1986. Grasp size and accuracy of approach in reaching. J. Mot. Behav. 18 (3), 245–260. https://doi.org/10.1080/00222895.1986.10735380.